Available online at www.sciencedirect.com
SCIENCE DIRECT®

Journal of the European Ceramic Society 23 (2003) 1911–1917
www.elsevier.com/locate/jeurceramsoc

Electrical conductivity of hexagonal $Ba(Ti_{0.94}Ga_{0.06})O_{2.97}$ ceramics

M.J. Rampling[a], G.C. Mather[b], F.M.B. Marques[c], D.C. Sinclair[a,*]

[a]*Department of Engineering Materials, Sir Robert Hadfield Building, University of Sheffield, Mappin Street, Sheffield S1 3JD, UK*
[b]*Instituto de Cerámica y Vidrio, Consejo Superior de Investigaciones Científicas, Campus de Cantoblanco, Camino de Valdelatas, Madrid, 28049, Spain*
[c]*Department of Ceramics and Glass Engineering, UIMC, University of Aveiro, 3810 Averio, Portugal*

Received 10 June 2002; received in revised form 24 October 2002; accepted 8 November 2002

Abstract

Impedance spectroscopy is used to estimate the bulk conductivity, σ_b, of hexagonal (6H)-$Ba(Ti_{0.94}Ga_{0.06})O_{2.97}$ ceramics in air, N_2 and $5\%H_2/95\%N_2$ between 400 and 1000 °C. Isothermal plots of log σ_b vs log pO_2 in the temperature range between 700 and 1000 °C show the presence of a p–n transition with slopes of $\sim -1/4$ and $+1/4$ in the n- and p-type regions indicating that the conductivity obeys the 'extrinsic' model proposed by Smyth and co-workers for undoped and acceptor-doped cubic $BaTiO_3$-based materials [*J. Am. Ceram. Soc.* 64 (1981) 556; *J. Am. Ceram. Soc.* 65 (1982) 167]. The activation energy E_a for oxidation in the p-type region to produce free holes is similar for 6H-$Ba(Ti_{0.94}Ga_{0.06})O_{2.97}$ and cubic $BaTiO_3$-based ceramics with an estimated value from σ_b data of $\sim$0.8 eV. The band gap for 6H-$Ba(Ti_{0.94}Ga_{0.06})O_{2.97}$ ceramics is $\sim$3.2 eV.

Keywords: $BaTiO_3$; Electrical conductivity; Impedance spectroscopy

1. Introduction

Barium titanates have long been recognised as good dielectric materials and are commonplace in the electroceramics market. For example, tetragonal $BaTiO_3$ (t-$BaTiO_3$) is a ferroelectric material that can exhibit exceptionally large permittivity values, ca. 10,000 at the tetragonal to cubic (c-$BaTiO_3$) phase transition making it an important dielectric material for ceramic capacitors. The defect chemistry of undoped c-$BaTiO_3$ has been investigated by several techniques including the dependence of the electrical conductivity, σ, on oxygen partial pressure, pO_2, at temperatures >600 °C.[1] With increasing pO_2, σ changes from being n-type to p-type at $\sim 10^{-1}$–10^{1} Pa and three distinct regions are observed. At very low pO_2 in the n-type region, σ is proportional to $pO_2^{-1/6}$ (region I), at intermediate pO_2 the conductivity is proportional to $pO_2^{-1/4}$ (region II) and at high pO_2 in the p-type region, σ is proportional to $pO_2^{+1/4}$ (region III). There is a conductivity minimum between the n- and p-type regions which shifts to higher pO_2 with increasing temperature.

Chan et al.[1] have modelled the conductivity behaviour of undoped c-$BaTiO_3$ ceramics in terms of the so-called 'extrinsic' model where the p-type behaviour below $\sim$1000 °C and $pO_2 > 10^0$ Pa is attributed primarily to the presence of unavoidable aliovalent impurities (such as Al from the reagent grade TiO_2) of valence $< +4$ on the Ti-sites. These defects are often called acceptor impurities and are charge compensated by a corresponding number of oxygen vacancies, $V_O^{\bullet\bullet}$ in the $BaTiO_3$ lattice. According to this model, the full condition of charge neutrality is

$$[A'] + n = 2[V_O^{\bullet\bullet}] + p \quad (1)$$

where [A′] is the summation of all acceptor states present and n and p are the concentration of electrons, [e′] and holes, [h•]. At low pO_2 in the n-type region, the following reduction reaction dominates

$$O_O^x \Rightarrow 1/2O_2 + V_O^{\bullet\bullet} + 2e' \quad (2)$$

with a mass-action expression

$$[V_O^{\bullet\bullet}]n^2 = K_r pO_2^{-1/2} \quad (3)$$

* Corresponding author. Tel.: +44-114-222-5974; fax: +44-114-222-5943.
E-mail address: d.c.sinclair@sheffield.ac.uk (D.C. Sinclair).

0955-2219/03/$ - see front matter © 2003 Elsevier Science Ltd. All rights reserved.
doi:10.1016/S0955-2219(02)00448-X

where K_r is the mass action constant for the reduction reaction. In region I, at low pO_2 the charge neutrality condition is

$$n \approx 2[V_O^{\bullet\bullet}] \quad (4)$$

and substitution of (4) into (3) shows n and therefore conductivity to be proportional to $pO_2^{-1/6}$. In region II, the charge neutrality condition is

$$[A'] \approx 2[V_O^{\bullet\bullet}] \quad (5)$$

and substitution of (5) into (3) shows n and therefore conductivity to be proportional to $pO_2^{-1/4}$.

At high pO_2 in the p-type region, the following oxidation reaction occurs

$$V_O^{\bullet\bullet} + 1/2O_2 \Rightarrow O_O^x + 2h \quad (6)$$

with a mass-action expression

$$p^2 = K_o[V_O^{\bullet\bullet}]pO_2^{1/2} \quad (7)$$

where K_o is the mass action constant for the oxidation reaction. In region III, the charge neutrality condition is given in Eq. (5) and combining (5) and (7) shows p and therefore conductivity to be proportional to $pO_2^{+1/4}$ (providing only a minor fraction of the impurity-related $V_O^{\bullet\bullet}$ is filled). The availability of $V_O^{\bullet\bullet}$ created by the acceptor-type impurities provides an easy mechanism to account for the unexpected p-type behaviour in undoped c-$BaTiO_3$.[1]

In this model, intrinsic behaviour is observed only in region I; the conductivity behaviour in regions II and III is dominated by [A′]. The oxidation and reduction regimes are separated by a conductivity minimum, σ_{min}, that corresponds to a p–n transition and represents the intrinsic conductivity associated with thermal generation of charge carriers across the band gap, according to the equation

$$nil \Rightarrow e' + h^{\bullet} \quad (8)$$

where nil is the thermodynamic standard state, defined as the 'perfect' crystal with all electrons in the lowest available energy state.[1] The mass action expression for this reaction is

$$np = K_i \quad (9)$$

where K_i is the mass action expression for this ionisation reaction.

This model has led to values of 0.92 eV for the enthalpy of oxidation to form free holes [Eq. (6)], 5.96 eV for the enthalpy of reduction [Eq. (2)] and a band gap of ~3.14 eV (Eq. (8)]. Two additional features have been incorporated to this model to account for deviations from experimental observations. First, the conductivity in the vicinity of the p–n transition is higher than expected and is insensitive to pO_2. This has been attributed to ionic conduction associated with $V_O^{\bullet\bullet}$. Second, the derived acceptor content in lightly-Al-doped samples is less than expected[2] and shows a slight decrease with decreasing temperature. This has been attributed to trapping of the holes by the acceptors at lower temperatures, according to the reaction

$$A' + h^{\bullet} \Rightarrow A^x \quad (10)$$

The enthalpy of oxidation associated to form trapped holes has been determined to be −0.15 eV,[2] indicating that the concentration of trapped holes decreases with increasing temperature. The increase in p-type conductivity with increasing temperature is therefore attributed to increasing ionisation of a decreasing population of trapped holes.

$BaTiO_3$ has various polymorphs, all of which are based on the perovskite structure (ABO_3); however, due to its high permittivity, ferroelectric t-$BaTiO_3$-based materials have received the most attention. Surprisingly, very little is known about the electrical properties and defect chemistry of the high temperature hexagonal (6H) polymorph which is stable above 1460 °C in undoped $BaTiO_3$.[3] In part this is due to undoped hexagonal $BaTiO_3$ being metastable at room temperature. The 6H-$BaTiO_3$ structure which has been reported as space group $P6_3/mmc$ is shown in Fig. 1 and can be described in terms of close packed BaO_3 layers, with a $[cch]_2$ sequence, i.e. $[Ba(2)O(2)_3Ba(2)O(2)_3Ba(1)O(1)_3]_2$.[4] Atoms Ti(1) and Ti(2) occupy corner- and face-sharing octahedra respectively, with rather short Ti(2)–Ti(2) distances in the face sharing Ti_2O_9 octahedra.

Recently we have been investigating chemical doping of $BaTiO_3$ to obtain the hexagonal (6H) polymorph at room temperature. Here we present results of an impedance spectroscopy study on Ga-doped $BaTiO_3$ ceramics that exhibit the 6H-$BaTiO_3$ structure at room temperature. The conductivity has been studied over the range ~400–1000 °C between $10^{-20} < pO_2 < 10^4$ Pa and the results are compared with those for undoped c-

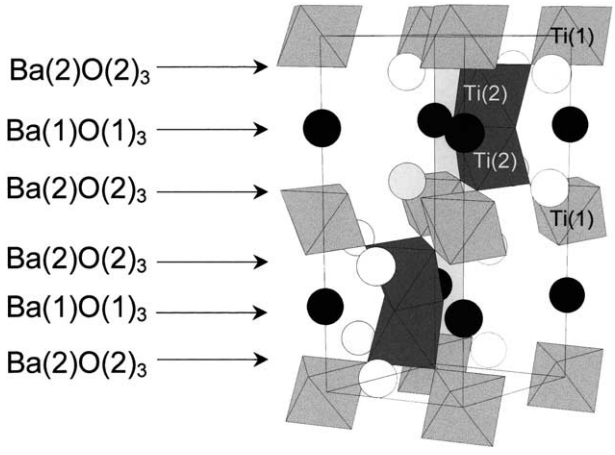

Fig. 1. The crystal structure of 6H-$BaTiO_3$. Black and white symbols represent Ba(1) and Ba(2), respectively, light and dark shaded octahedra represent $Ti(1)O_6$ and $Ti(2)O_6$, respectively. For clarity O^{2-} ions are not shown.

$BaTiO_3$ ceramics based on the 'extrinsic' model developed by Smyth and co-workers.[1,2]

2. Experimental

Appropriate quantities of $BaCO_3$, TiO_2 and Ga_2O_3 (Aldrich, all +99.99 pure) were weighed (5–8 g) to give a formula $BaTi_{0.94}Ga_{0.06}O_{2.97}$ and intimately mixed in acetone in an agate mortar and pestle until dry. The mixed powder was placed on a Pt boat and fired in air. Firing schedules were 1000 °C for 2 h to decarbonate, and 1350 °C for 3 days, with daily regrinding in acetone in an agate mortar and pestle.

X-ray diffraction (XRD) using a Hagg-Guinier camera with Cu $K_{\alpha 1}$ radiation of wavelength 1.5418 Å was used to follow the progress of the reaction and as a first indicator of phase purity. Lattice parameters were calculated using data obtained from a Stoe Stadi P diffractometer which was calibrated using an external Si standard. Pellets were prepared by uniaxial pressing of powders to 300 MPa in an 8 mm stainless steel die. The green bodies were sintered on Pt foil overnight at 1350 °C in air. Pellet densities were calculated using pellet mass and dimensions and were expressed as a percentage of the theoretical X-ray density.

Microstructural properties such as grain size distribution and morphology were determined using a Camscan (MK2, Oxford Instruments) electron microscope operating at 20 kV. Samples were in the form of fractured pellets. These were mounted on an Al stub and gold coated to avoid charging under the beam.

Pellets for impedance measurements were prepared as above. Electrodes were fabricated from Pt organopaste and Pt foil; electroded pellets were fired to 1000 °C for an hour to remove organics to harden the Pt paste and to attach the Pt foil to the pellet faces. Two terminal impedance measurements were performed in a controlled-atmosphere furnace equipped with a type-B thermocouple and a Yttria-stabilised ZrO_2 (YSZ) sensor with Pt electrodes attached to an external voltmeter; the YSZ sensor was placed adjacent (<1 cm) to the sample to avoid inaccurate pO_2 readings as a result of oxygen fugacity fronts between the sensor and sample.[5] Measurements were first performed over the temperature range ~400–1000 °C in air, then N_2 and finally in $5\%H_2/95\%N_2$ across the frequency range 20 Hz–1 MHz using an HP4192 impedance analyser with an applied voltage of 100 mV. On changing the atmosphere from air to N_2, or from N_2 to $5\%H_2/95\%N_2$ the sample was equilibrated at 1000 °C. After equilibrium had been attained at 1000 °C (~12–15 h to obtain a constant dc conductivity), measurements were performed down to ~400 °C in steps of ~50 °C. Below ~400 °C the samples were too resistive ($>10^8$ Ω) to measure using the impedance analyser. After a cooling and heating cycle in $5\%H_2/95\%N_2$ had been completed, data were collected at temperatures of 1000, 900, 800 and 700 °C over a range of pO_2 regimes by first equilibrating the furnace in reducing atmosphere ($5\%H_2/95\%N_2$) then switching off the reducing gas and allowing a slow leak of O_2 into the furnace, thereby allowing isothermal measurements to be taken in the approximate ranges $pO_2 < 10^{-8}$ Pa and $>10^2$ Pa. Within these temperature-dependent pO_2 limits (the lambda gap), impedance data could not be collected at accurately determined pO_2 values with our experimental set-up as a result of the well-documented saturation effect associated with YSZ potentiometric sensors in this intermediate pO_2 range.[5]

3. Results

The X-ray diffraction pattern for $Ba(Ti_{0.94}Ga_{0.06})O_{2.97}$ powder is shown in Fig. 2 and fully indexed on the hexagonal cell reported in ICDS file 34-129. The lattice parameters were $a = 5.7244(3)$ and $c = 13.9949(7)$ Å and $V = 397.16(3)$ Å^3 compared with $a = 5.72481(11)$ and $c = 13.9673(3)$ Å and $V = 396.4(4)$ Å^3 for undoped 6H-$BaTiO_3$. The solid solution limits and refinements of powder X-ray and Neutron diffraction data for the single-phase 6H-$Ba(Ti_{1-x}Ga_x)O_{3-x/2}$ solid solution will be discussed in detail elsewhere.[6]

Pellet densities were estimated to be ~85% of the theoretical X-ray density and SEM micrographs of the ceramic microstructure revealed the presence of open porosity with an average grain size between 3 and 5 μm, as shown in Fig. 3.

The impedance response of the ceramics could be modelled on an equivalent circuit consisting of two parallel RC elements connected in series and conductivity values were extracted from impedance complex plane plots, Z^*. Typical data are shown in Fig. 4 and consist of two arcs with approximate capacitances (calculated from $\omega RC = 1$ at their maxima) of ~10

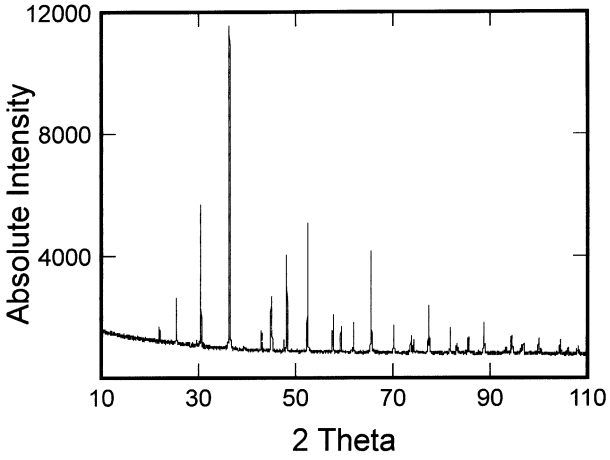

Fig. 2. X-ray diffractogram of 6H-$BaTi_{Ø.94}Ga_{0.06}O_{2.97}$.

pFcm^{-1} and ~20 nFcm^{-1}. The first value (associated with the large, higher-frequency arc) is a typical bulk value whereas the second capacitance (associated with the small, lower-frequency arc) is a typical grain boundary value. Hence, the bulk resistance, R_b, was taken as the intercept of the higher frequency arc on the real, Z', axis and the bulk conductivity, $\sigma_b = 1/R_b$. Z'' and M'' spectroscopic plots (where $M^* = j\omega C_o Z^*$ and $j = \sqrt{-1}$ and C_0 is the vacuum capacitance of the cell) both showed the presence of a single Debye-like peak with a similar value of ω_{max}, Fig. 5. Spectroscopic plots of M'' data are dominated by small capacitances and therefore highlight the bulk response, whereas spectroscopic plots of Z'' data highlight the most resistive element in the ceramic.[7] Plots such as Fig. 5 confirm the high frequency arc in Z^* plots to be the bulk response and also confirm the dc resistance of the pellets to be dominated by the bulk component. (At all temperatures measured the grain boundary resistance was ~2 orders of magnitude smaller than the bulk resistance)

Arrhenius plots of σ_b for samples measured in air, N_2 and 5%H_2/95%N_2 are shown in Fig. 6. Changing the atmosphere from air ($pO_2 \sim 10^4$ Pa) to N_2 ($pO_2 \sim 10$ Pa) shows a decrease in conductivity indicative of p-type conductivity, whereas there is a substantial increase in the conductivity for ceramics equilibrated in 5%H_2/95%N_2 ($pO_2 \sim 10^{-20}$ Pa at 1000 °C), indicative of n-type conduction. The activation energy associated with the bulk conductivity is similar in air and N_2 with a value of ~0.80(2) eV, whereas in the n-type region it is higher with a value of ~1.11(3) eV. It should be noted, however, that the results obtained in the n-type region are not at a fixed pO_2 as it is well documented that pO_2 depends strongly on temperature for H_2/N_2 gas compositions.

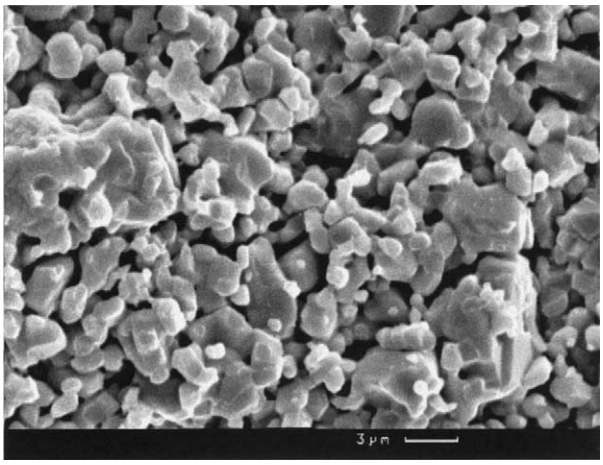

Fig. 3. SEM micrograph of a fracture surface of a 6H-$BaTi_{Ø.94}Ga_{0.06}O_{2.97}$ ceramic.

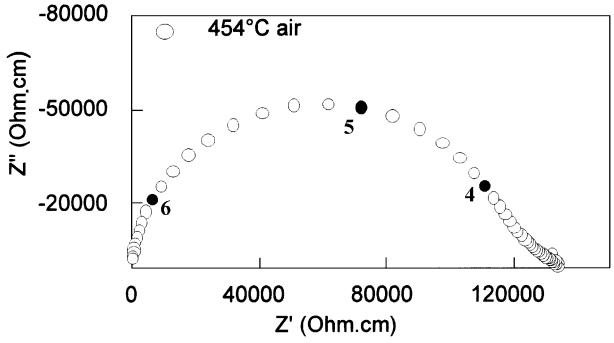

Fig. 4. Z^* plot at 454 °C. Selected frequencies (in Hz) are shown by filled circles on a log scale, e.g. 6 = 10^6 Hz.

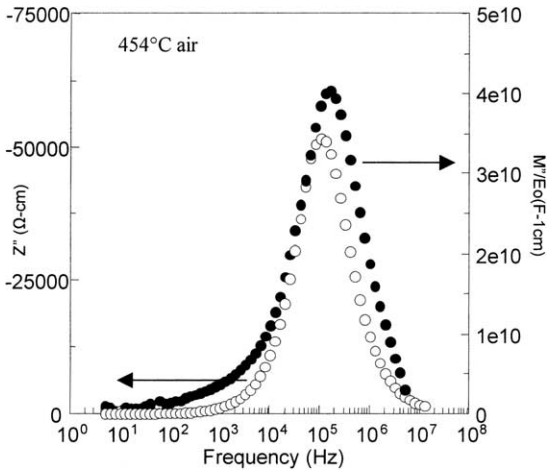

Fig. 5. Combined Z'' and M'' spectroscopic plot at 454 °C.

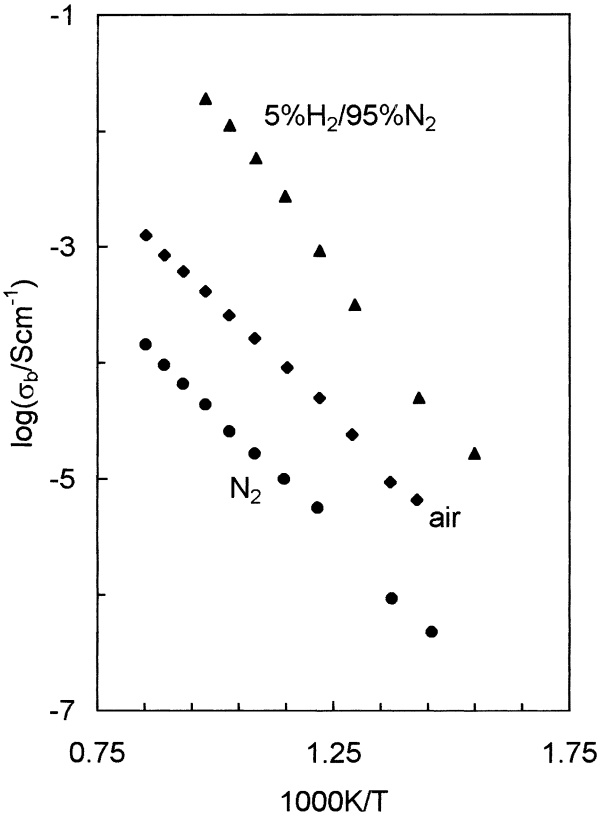

Fig. 6. Arrhenius plot of σ_b in air, N_2 and 5%H_2/95%N_2.

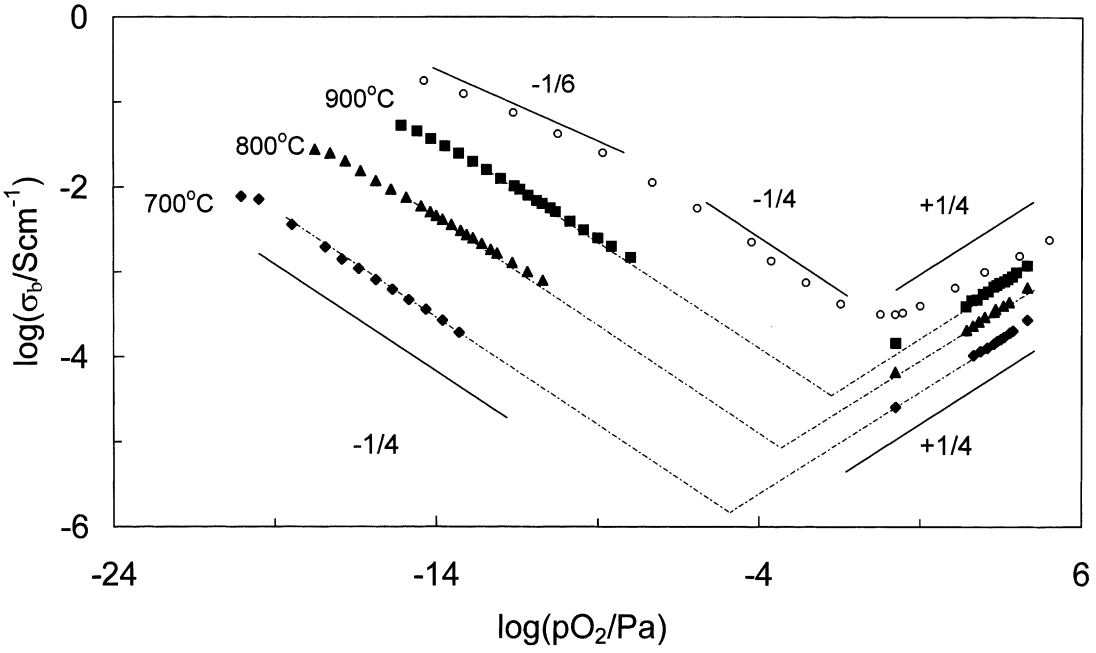

Fig. 7. Log σ_b vs log pO_2 for 700–900 °C for 6H-$BaTi_{0.94}Ga_{0.06}O_{2.97}$ ceramics (filled symbols). Open symbols are data from Ref. [1] for undoped c-$BaTiO_3$ at 900 °C.

The pO_2 dependence of σ_b was studied in more detail by performing isothermal oxidation runs from the low pO_2 associated with the $5\%H_2/95\%N_2$ atmosphere at temperatures between 700 and 1000 °C. The results show n-type behaviour for σ_b with a slope of $\sim -1/4$ at low pO_2 and p-type behaviour at high pO_2 with a slope of $\sim +1/4$, Fig. 7. Least square fits to the data for the various temperatures and regions are summarised in Table 1. For comparison, conductivity values for undoped c-$BaTiO_3$ ceramics at 900 °C from the work of Smyth and co-workers[1] are included in Fig. 7. Unfortunately our experimental set-up does not permit reliable values of pO_2 to be obtained in the intermediate region of pO_2 associated with the p–n transition. Accurate values for the minimum in σ_b, $\sigma_{b,min}$, could not be established directly by experiment; however, they were estimated by the intersection of straight line extrapolations of the data from the n- and p-type regions, Fig. 7. An Arrhenius plot of extrapolated $\sigma_{b,min}$ values against temperature for 6H-$Ba(Ti_{0.94}Ga_{0.06})O_{2.97}$ ceramics is shown in Fig. 8, along with $\sigma_{b,min}$ data for undoped c-$BaTiO_3$ ceramics.[1,8] The slopes of the plots are similar with an E_a value of ~ 1.60 eV.

Table 1
Slope values from Fig. 7

Temperature/°C	n	p
700	−0.24(3)	+0.25(3)
800	−0.23(3)	+0.25(3)
900	−0.22(3)	+0.23(3)
1000	−0.22(3)	+0.23(3)

4. Discussion

Ga^{3+} has an ionic radius of 0.62 Å which is close to the value of 0.605 Å reported for Ti^{4+}.[9] The room temperature stabilisation of the hexagonal polymorph, Fig. 2 is therefore presumably related to the presence of oxygen vacancies in the structure as opposed to a small size effect associated with Ga^{3+} substitution. Detailed structural characterisation will be reported elsewhere.[6]

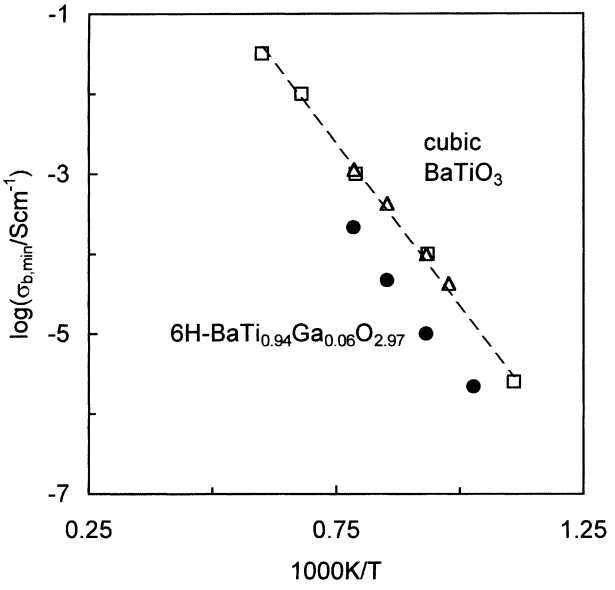

Fig. 8. Arrhenius plot of $\sigma_{b,min}$ for 6H-$BaTi_{0.94}Ga_{0.06}O_{2.97}$ ceramics (filled symbols). Open symbols (squares and triangles) are data from Ref. [1,8] for undoped c-$BaTiO_3$, respectively.

However, Reitveld refinement of powder neutron diffraction data show replacement of Ti by Ga to be accompanied by the formation of O(1) oxygen vacancies in the h-$Ba(1)O(1)_3$ layers which separate pairs of occupied face-sharing octahedra, $Ti(2)_2O_9$. There is no evidence of O(2) vacancies associated with corner sharing TiO_6 octahedra. The small increase in unit cell volume and c/a ratio from 2.439 to 2.444 for 6H-$Ba(Ti_{0.94}Ga_{0.06})O_{2.97}$ compared to undoped 6H-$BaTiO_3$ is attributed primarily to increased cation-cation repulsion between the face-sharing octahdera as there is less shielding between the cations from O(1) ions, Fig. 1.

It is well known that dense $BaTiO_3$-based ceramics require long equilibration periods with the gas ambient below 1000 °C to obtain 'equilibrium' conductivity values.[1] In an attempt to circumvent this problem and improve the equilibration characteristics the ceramic microstructure of the 6H-$Ba(Ti_{0.94}Ga_{0.06})O_{2.97}$ pellets was deliberately engineered to produce bodies of low pellet density and small average grain size, as shown in Fig. 3. Conductivity studies in air of dense ceramics (~95% of the theoretical density) showed similar values to that presented here for pellets with ~85% of the theoretical X-ray density demonstrating that porosity did not have a deleterious effect on the magnitude of the bulk conductivity. Results of isothermal oxidation experiments from reducing atmospheres on dense pellets; however, showed the conductivity in the n-type region to have a pO_2 dependence $<-1/6$, suggesting that equilibration of dense ceramics with the gas ambient was incomplete for our experimental set-up. This justifies the use of porous ceramics to study the high temperature conductivity behaviour of 6H-$BaTi_{0.94}Ga_{0.06}O_{2.97}$ ceramics as a function of pO_2.

Impedance spectroscopy showed the conductivity of the ceramics to be dominated by the bulk component over the measured T-pO_2 range, Figs. 4 and 5. This is in contrast to undoped c-$BaTiO_3$ ceramics where the grain boundary component can dominate the impedance response, especially in the p-type region at temperatures <850 °C.[10] The absence of a resistive grain boundary component in dense (~95% of the theoretical X-ray density) 6H-$Ba(Ti_{0.94}Ga_{0.06})O_{2.97}$ ceramics (not shown) suggests that grain boundary impedances are not associated simply with pellet density and that a rather complex interplay between ceramic and electrical microstructure exists for cubic and hexagonal $BaTiO_3$-based materials. Arrhenius plots of the bulk conductivity for porous 6H-$Ba(Ti_{0.94}Ga_{0.06})O_{2.97}$ ceramics in air, N_2 and 5%H_2/95%Ar shown in Fig. 6 indicate the presence of a change in conduction mechanism from p-type to n-type behaviour at a pO_2 intermediate between flowing N_2 and 5%H_2/95%N_2. On the assumption that the bulk conductivity is proportional to the carrier concentration, E_a in the p-type region is similar for air and N_2 and the value of ~0.80 eV is in reasonable agreement with that reported for undoped c-$BaTiO_3$. Although this treatment does not take into account hole mobility, this value of ~0.80 eV for the production of free holes, Eq. (6), is in reasonable agreement with the value of 0.92 eV obtained from calculations by Smyth et al from conductivity data on undoped[1] and Al-doped c-$BaTiO_3$ ceramics.[2]

Fig. 7 confirms the presence of a p–n transition in 6H-$Ba(Ti_{0.94}Ga_{0.06})O_{2.97}$ ceramics and the observed slopes of $-1/4$ and $+1/4$ for the isothermal log σ_b vs log pO_2 plots indicate extrinsic behaviour over the measured T and pO_2 ranges, with the electroneutrality condition $2[V_O^{\cdot\cdot}]=[Ga']$. Given the large concentration of acceptor states present, extrinsic behaviour is expected and the results are qualitatively consistent with the defect model proposed by Smyth et al. for undoped and Al-doped c-$BaTiO_3$.[1,2] As expected, the p–n transition is suppressed to lower pO_2 compared to undoped c-$BaTiO_3$ ceramics due to the higher acceptor-state content in the Ga-doped samples; however, the Ga-doped samples have slightly lower conductivity in the p-type region, Fig. 7.

Smyth et al. have shown that the band gap, E_g^o, can be estimated from an Arrhenius plot of $\sigma_{b,min}$, as $E_g=2E_a$. They reported a value of $E_g^o \sim 3.2$ eV for undoped and Al-doped c-$BaTiO_3$. Fig. 8 shows their data and also data from Seuter[8] along with the extrapolated values of $\sigma_{b,min}$ for 6H-$Ba(Ti_{0.94}Ti_{0.06})O_{2.97}$ ceramics: all the data sets give similar E_a's of ~1.6 eV. This leads to the conclusion that the band gap in 6H-$BaTi_{0.94}Ga_{0.06}O_{2.97}$-based ceramics is ~3.2 eV and is similar to that of c-$BaTiO_3$-based ceramics.

5. Conclusions

Single-phase powder and ceramics of $Ba(Ti_{0.94}Ga_{0.06})O_{2.97}$ that crystallise in the 6H-$BaTiO_3$ structure can be prepared from the mixed oxide route in air at 1350 °C. Stabilisation of the 6H structure is attributed to the presence of oxygen vacancies in the $Ba(1)O(1)_3$-layers between the face sharing Ti_2O_9 octahedra as opposed to a difference in cation size associated with partial replacement of Ti^{4+} with Ga^{3+} ions. Impedance spectroscopy shows the resistance of 6H-$Ba(Ti_{0.94}Ga_{0.06})O_{2.97}$ ceramics to be dominated by the bulk component. This is in contrast to c-$BaTiO_3$-based ceramics where the resistance is normally dominated by a resistive grain boundary component, especially for measurements conducted in air.[10]

logσ_b vs log pO_2 data confirm the presence of a p–n transition in 6H-$Ba(Ti_{0.94}Ga_{0.06})O_{2.97}$ ceramics. Slopes of $\sim -1/4$ and $+1/4$ are obtained in the n- and p-type regions, respectively, and are consistent with that expected from the 'extrinsic' defect model proposed by Smyth and co-workers for acceptor doped c-$BaTiO_3$.[2] A

change to a slope of $-1/6$ at very low pO_2 is not observed for the 6H-$Ba(Ti_{0.94}Ga_{0.06})O_{2.97}$ ceramics, presumably due to the large concentration of Ga^{3+} ions. The activation energy E_a for oxidation in the p-type region to produce free holes is similar in 6H-$Ba(Ti_{0.94}Ga_{0.06})O_{2.97}$ and c-$BaTiO_3$-based ceramics with an estimated value from bulk conductivity measurements of $\sim$0.8 eV. An Arrhenius plot of estimated $\sigma_{b,min}$ values for 6H-$Ba(Ti_{0.94}Ga_{0.06})O_{2.97}$ ceramics reveals a band gap of $\sim$3.2 eV, a value similar to that obtained for c-$BaTiO_3$-based materials. To our knowledge, this is the first estimation of the band gap for a 6H-$BaTiO_3$-based material.

Acknowledgements

We thank the EPSRC (studentship to M.J.R.), ERASMUS and FTC (Portugal) for financial support during this research. D.C.S. would also like to thank The Royal Society of Chemistry for a J.W.T. Jones Travel Fellowship.

References

1. Chan, N.-H., Sharma, R. K. and Smyth, D. M., Nonstoichiometry in undoped $BaTiO_3$. *J. Am. Ceram. Soc.*, 1981, **64**, 556–562.
2. Chan, N.-H., Sharma, R. K. and Smyth, D. M., Nonstoichiometry in acceptor-doped $BaTiO_3$. *J. Am. Ceram. Soc.*, 1982, **65**, 167–170.
3. Kirby, K. W. and Wechsler, B. A., Phase relations in the Barium titanate-titanium oxide system. *J. Am. Ceram. Soc.*, 1991, **74**, 1841–1947.
4. Akimoto, J., Gotoh, Y. and Oosawa, Y., Refinement of H-$BaTiO_3$. *Acta. Crystallogr.*, 1994, **C50**, 160–162.
5. Marques, F. M. B. and Wirtz, G. P., Oxyen fugacity control in nonflowing atmospheres.I. experimental-observations in CO/CO_2 and O_2/N_2. *J. Am. Ceram. Soc.*, 1992, **75**, 369–374.
6. Rampling, M. J., Keith, G. M., Kirk, C. A., and Sinclair, D. C. Unpublished results.
7. Sinclair, D. C. and West, A. R., Impedance and modulus spectroscopy of semiconducting $BaTiO_3$ showing positive temperature coefficient of resistance. *J. Appl. Phys.*, 1988, **66**, 3850–3856.
8. Seuter, A. M. J. H., Defect chemistry and electrical properties of barium titanate. *Philips Res. Rep.*, 1974, **3**, 51–65.
9. Shannon, R. D., Ionic radii. *Acta. Crystallogr.*, 1976, **A32**, 751–767.
10. Clark, I. J., Marques, F. M. B. and Sinclair, D. C., The influence of grain boundary impedances on the p-type behaviour of undoped $BaTiO_3$ ceramics. *J. Eur. Ceram. Soc.*, 2002, **22**, 579–583.